Inward and outward membrane tubes pulled from giant vesicles

Fast Track Communication

Inward and outward membrane tubes pulled from giant vesicles

Raktim Dasgupta and Rumiana Dimova

Department of Theory and Bio-Systems, Max Planck Institute of Colloids and Interfaces, Science Park Golm, 14424 Potsdam, Germany

E-mail: raktim.dasgupta@mpikg.mpg.de, dimova@mpikg.mpg.de

Abstract

Membrane nanotubes are extruded from giant unilamellar lipid vesicles using a controlled hydrodynamic flow and membrane-attached beads manipulated via optical tweezers. Within a single experiment, the technique can be used to assess various important mechanical and rheological characteristics of the membrane such as the bending rigidity, tension and intermonolayer slip. The application of small flow velocities leads to the extrusion of tubes with sufficiently large diameters conveniently measurable under an optical microscope. For the first time, we show that by suitably controlling the medium flow, inward tubes inside the vesicles can be formed. This approach offers great potential for studying tubulation mechanisms in membrane systems, exhibiting positive as well as negative spontaneous curvatures and should offer a more realistic model for biomembranes because the vesicle membrane tension can adapt freely.

Keywords: membrane tubes, optical trapping, membrane tension, bending rigidity, intermonolayer slip

(Some figures may appear in colour only in the online journal)

Biomembranes are very flexible and can easily bend to adopt the shapes of thin elongated cylinders, known as membrane tubes or tethers. Such structures commonly occur in cells [1] and are involved in a large number of important cellular functions such as cell migration [2], intercellular trafficking [3], intracellular trafficking [4] and signalling [5]. Because biological membranes are fairly complex systems, model membrane systems have been explored to understand the mechanisms driving cellular processes. Among them, giant unilamellar lipid vesicles (GUVs) [6, 7] have become very popular because they can be used to visualize the membrane directly under an optical microscope. Membrane tubes have been pulled out of GUVs employing a wide range of approaches based on the use of hydrodynamic flows [8–11], gravity [12], micromanipulation [8, 13, 14], magnetic or optical tweezers [15–17]. Tube pulling experiments provide a convenient method to study membrane elastic properties and to understand how the bilayer structure and composition can influence membrane behaviour. Tube formation is now conventionally applied for studying membrane curvature sorting and sensing of proteins, see e.g. [18]. Apart from mimicking several biological phenomena, tube extraction in GUVs also finds applications in the fabrication of tube-based networks for nanofluidic devices and in artificial cell design [19].

Among the different techniques used for pulling tubes from lipid membranes, the more widely used approach involves the use of a pipette to aspirate the vesicle, from which a tube is pulled out. In this case, the membrane tension is preset and kept constant by the suction pressure of the aspirating micropipette. However, in cells, the membrane tension may vary and adjust according to the membrane reshaping process and even modulate this very process [20, 21]. Furthermore, since the technique essentially requires aspirating the vesicle

J. Phys. D: Appl. Phys. **47** (2014) 282001

Fast Track Communication

using a pipette and therefore presetting the membrane tension, it cannot be used to study the response of the membrane to changes in its tension. The need to hold the vesicle via aspiration by itself imposes a minimal tension, below which experiments cannot be performed, limiting the accessible tension range. One approach, for which the membrane tension can vary during the tube formation, is provided by the use of hydrodynamic flows to pull membrane tubes. Tube extrusion has been achieved by using hydrodynamic forces from sedimenting vesicles [11] or from vesicles with an attachment point on either a glass substrate [8] or a micro-rod [9]. However, these experimental scenarios are inherently restrictive compared to an approach combining hydrodynamic flows and magnetic or optical traps as used here. This latter approach allows us to reach the full potential of estimating various elastic properties of the lipid vesicles.

It is also pertinent to note that up to now, all tube pulling experiments report the extrusion of only outward tubes from the vesicle membrane. This approach is suitable for investigating the effect of molecules, which generate positive spontaneous curvature (i.e. outward bending) in the membrane when added to the vesicle exterior. For molecules inducing inward membrane bending, i.e. negative spontaneous curvature, such as I-BAR proteins, which have been shown to induce internal vesicle tubulation [22], pulling inward tubes in giant vesicles would be advantageous.

Here, we show that membrane tubes extruded under hydrodynamic flows with the help of optical tweezers can be used to obtain various important mechanical and rheological characteristics of the membrane within a single experiment. Our approach starts with the formation of outward tubes. A vesicle was brought into contact with an optically trapped bead and thereafter dragged away from the bead by a controlled hydrodynamic flow. No preset tension on the vesicles needed to be applied and the vesicles were predominantly being acted upon by very small tensions corresponding to the entropic regime. Thus, under slow flow velocities, this method offers formation of tubes with sufficiently large diameters (above the optical resolution limit) which could be directly measured. At higher flow velocities, thinner tubes could be formed. By suitably accounting for the hydrodynamic drag on the vesicle and studying the statics and dynamics of the tube pulling forces, we could assess several important material properties of the lipid membrane within a single experiment. We could also use the approach to manipulate a bead towards the vesicle interior. Once attached to the membrane, we could employ the trapped bead to pull inward tubes into the vesicle. This technique offers significant potential for studying processes promoting negative curvature in lipid membranes.

For vanishing spontaneous curvature, the tube pulling force can be written as [23],

$$f(t) = f_s(t) + bh^2 \ln\left(\frac{R_v}{R_c}\right) \dot{L}(t) \qquad (1)$$

where $L(t)$ is the length of the tube changing with time t and $\dot{L}(t)$ is the rate of change. The first term in this equation, the static pulling force $f_s(t)$, is given by

$$f_s(t) = 2\pi\sqrt{2\Sigma(t)\kappa} \qquad (2)$$

where $\Sigma(t)$ is the membrane tension and κ is the bending stiffness. The second term in equation (1) involves the friction between the two leaflets where b is the intermonolayer slip coefficient, h is the thickness of the hydrophobic bilayer, and R_v and R_c are the radii of the vesicle and the cylindrical tube, respectively. In equation (1), we have omitted the contribution of the restoring force opposing the asymmetry between the two membrane leaflets, arising from the unequal changes in their areas. This term is on the order of $\frac{\kappa}{2R_v^2}L(t)$ and is negligible in our experiments.

Neglecting the small changes in vesicle tension due to hydrodynamic friction [8], for a flaccid vesicle with initial tension Σ_0, the increasing tension during tube formation can be given as [24],

$$\frac{\Sigma(t)}{\Sigma_0} = \exp\left(\frac{8\pi\kappa}{k_B T}\frac{A_c(t)}{A_0}\right) \qquad (3)$$

where $A_c(t) = 2\pi R_c L(t)$ is the area of the cylindrical tube and $A_0 = 4\pi R_v^2$ is the surface area of the vesicle. When using hydrodynamic flow to extract a tube, the tube extrusion force increases with increasing length (as the vesicle is displaced). When the increased tension of the membrane counteracts the vesicle displacement with the flowing fluid, the vesicle becomes stationary. The maximum tension Σ_m reached at this point with flow velocity U, can thus be obtained from $6\pi\eta U R_v = 2\pi\sqrt{2\kappa\Sigma_m}$, i.e.

$$\Sigma_m = \frac{9\eta^2 U^2 R_v^2}{2\kappa}. \qquad (4)$$

Since $R_c(t) = \sqrt{\kappa/2\Sigma(t)}$, the corresponding tube radius at the maximum tension is

$$R_{cm} = \frac{\kappa}{3\eta U R_v}. \qquad (5)$$

Inserting the expression for Σ_m in equation (3), for the maximum tube length at the stationary state we have

$$L_m = \frac{3\eta k_B T R_v^3}{2\pi\kappa^2} U \ln\left(\frac{3\eta R_v}{\sqrt{2\kappa_0\Sigma_0}}U\right). \qquad (6)$$

At this point, when the medium flow is stopped the vesicle retracts towards the trapped bead and the tube shrinks in length. Note that during tube pulling and release, the vesicle size was not observed to change within the measurement error. The hydrodynamic drag acting on the retracting vesicle, $-6\pi\eta R_v\dot{L}(t)$, balances the mechanical force of the tube following

$$2\pi\sqrt{2\Sigma(t)\kappa} - bh^2\ln\left(\frac{R_v}{R_c}\right)\dot{L}(t) = -6\pi\eta R_v\dot{L}(t). \qquad (7)$$

Here the interleaflet friction acts to slow down the retraction process. Inserting Σ from equation (3) and neglecting the variation in R_c with time [24], the time evolution of a shrinking membrane tube can be described as

$$L(t) = -\frac{1}{M}\ln\left[\exp\left(-ML_m\right) + MNt\right] \qquad (8)$$

J. Phys. D: Appl. Phys. **47** (2014) 282001

Fast Track Communication

where $M = (2\pi\kappa R_c)/(k_B T R_v^2)$ and $N = \left(2\pi\sqrt{2\kappa_0\,\Sigma_0}\right)/\left(6\pi\eta R_v - bh^2\ln\left(R_v/R_c\right)\right)$.

For extrusion of membrane tubes oriented inward, we made use of hydrodynamic force to press the vesicle onto the bead and bring it to the vesicle interior. Once inside the vesicle, the trapped bead could be used to extrude tubes in a similar manner as used for pulling tubes outside the vesicle.

The experimental set-up [25] was built around a motorized inverted microscope (Axiovert 200 M, Zeiss) and comprises of single beam optical tweezers formed by focusing a 1064 nm, cw laser beam from a Nd : YAG laser (Spectra Physics, USA) through a $100\times$, NA 1.25 objective lens (Acroplan, Zeiss). The optical tweezers were used to trap streptavidin-coated polystyrene beads (Polyscience Inc) of $2 \pm 0.045\,\mu$m diameter and the trapping force was calibrated by applying varying viscous drag on the trapped sphere by movement of the motorized microscope stage (LStep13, Märzhäuser) and measuring the position of the trapped bead using the centroid tracking algorithm [26]. The precision of position sensing using the centroid tracking technique could be estimated to be $\sim$4 and $\sim$6 nm along the x and y directions, respectively. All measurements were performed at a height of $\sim$25 μm from the bottom glass boundary of the sample chamber. The stiffness of the tweezers was found to be $\sim$70.2 pN μm^{-1} W^{-1}. Typical laser powers used were $\sim$0.5 W at the sample.

Giant vesicles were grown at room temperature using the electroformation technique [27] in a solution of sucrose (100 mOsm) from 1-palmitoyl-2-oleoyl-sn-glycero-3-phosphatidylcholine (POPC) doped with 0.1 mol% biotinyl cap phosphatidylethanolamine (PE). All lipids were purchased from Avanti Polar Lipids. The biotinylated lipid serves to make vesicles adhere to the streptavidin-coated beads, which subsequently act as handles to pull the tubes. For better observations under the microscope and to facilitate streptavidin–biotin bonding, the vesicles were suspended in an isotonic medium of 40 mM glucose and 30 mM sodium chloride. All measurements were performed at $\sim$23 °C. Images were captured by an electron-multiplying charge-coupled device (EMCCD) camera (ImagEM, Hamamatsu Corp) at 30 frames per second. ImageJ was used for size and co-ordinate analysis of the vesicles using edge detection techniques [28].

When a flaccid vesicle was brought into contact with a trapped bead and subsequently dragged away by a hydrodynamic flow, a membrane tube could be seen to form at very low speeds of separation of a few μm s^{-1}. Interestingly, the tubes thus formed have diameters of a few hundred nm, conveniently measurable under optical microscope. This is unlike typically thin tubes with diameters of a few tens of nm formed from aspirated vesicle set under tension. Figure 1(*a*) shows a membrane tube pulled under a hydrodynamic flow $U \cong 10\,\mu$m s^{-1}. At that speed, the static tube length was 3.2 μm. For measuring the tube diameter we plotted the grey level distribution in the transverse section of the tube averaged over seven locations along its length (figure 1(*b*)). The data were fitted to a Gaussian [29], which gives the tube diameter for the vesicle shown as $2R_{cm} \cong 0.63\,\mu$m. Therefore, from equation (6), we could estimate the bending rigidity $\kappa =$
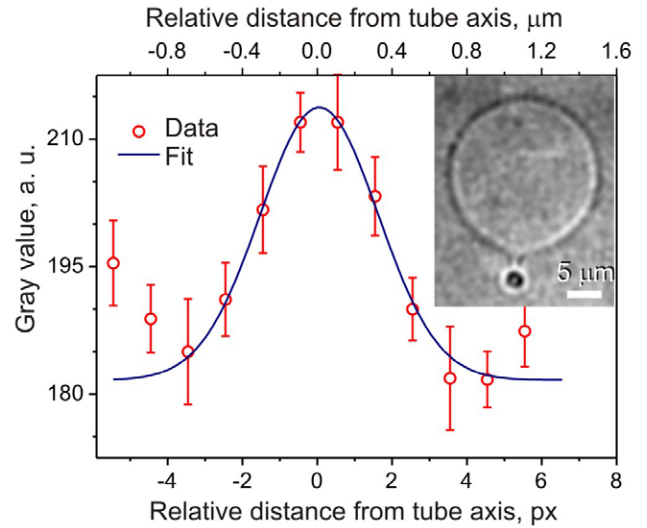

Figure 1. Optical determination of a tube diameter. An outward tube was formed upon subjecting a giant vesicle with diameter $2R_v \cong 21\,\mu$m to a flow with low velocity $U \cong 10\,\mu$m s^{-1}; see inset. Grey level distribution along the transverse section of the tube is fitted to a Gaussian fit (solid curve), see text for details. The data (open circles) present the mean of seven measurements at different locations and the error bars represent the standard deviations.

$(1.01\pm0.09)\times 10^{-19}$ J or $\kappa = 26\pm2k_B T$. The error represents the standard deviation over ten experiments. Measurements over five other vesicles yield $\kappa = (1.14 \pm 0.18) \times 10^{-19}$ J or $\kappa = 28 \pm 4k_B T$. These results are in good agreement with previous reports for POPC [30]. For the vesicle in figure 1, knowing κ we can also estimate the maximum membrane tension, $\Sigma_m \cong 5.1\times 10^{-7}$ N m^{-1} using equation (4) and taking $\eta = 1.015$ cP for the viscosity of 40 mM glucose solution [31]. The initial tension of the vesicle (before the tube was pulled) using equation (3) is $\Sigma_0 \cong 3.1 \times 10^{-8}$ N m^{-1}.

When the vesicle was subjected to changing hydrodynamic velocities, stationary membrane tubes of varying length could be formed (figure 2(*a*)). In figure 2(*b*), we have shown the measured lengths of tubes at varying flow velocities for a single vesicle (the same vesicle as in figure 1). The data represent the mean values of ten measurements at each flow speed. The measured values were fitted using equation (6) with κ and Σ_0 as fitting parameters (solid curve in figure 2(*b*)). It can be seen that the experimental data agree well with the predictions from equation (6). The best fit was obtained for $\kappa = 1.21 \times 10^{-19}$ J and $\Sigma_0 = 1.48 \times 10^{-8}$ N m^{-1}, values in good agreement with the estimate made from directly measuring the tube radius (figure 1). Similar measurements were carried out over five other vesicles yielding for the bending rigidity $\kappa \cong (1.22 \pm 0.25) \times 10^{-19}$ J or $(29 \pm 6)k_B T$.

From the theoretical curves in figure 2(*b*) and equation (6), it is evident that the formation of the membrane tube can be initiated at flow velocities as low as $\sim$3 μm s^{-1}, requiring a pulling force of only $\sim$0.5 pN. This value is about two orders of magnitude lower than the typical threshold needed when working with vesicles aspirated in a micropipette. This can be of significant advantage when studying membrane tubulation mechanisms. The use of such low forces expands

J. Phys. D: Appl. Phys. **47** (2014) 282001

Fast Track Communications

Fast Track Communication
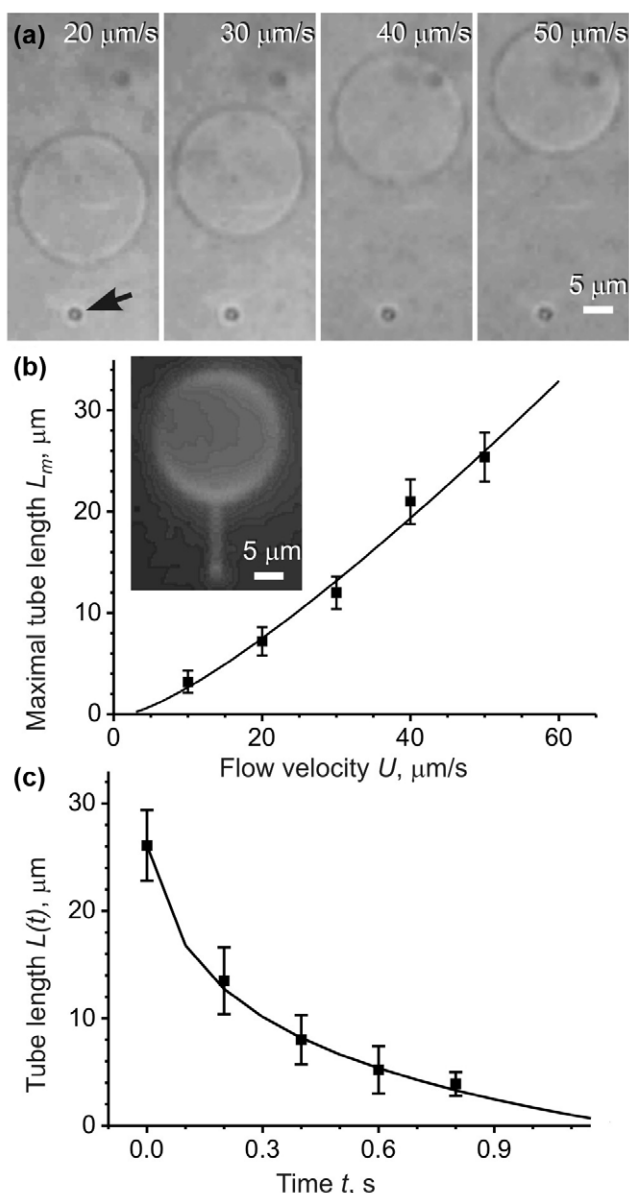
Figure 2. (a) The same vesicle as in figure 1 at stationary states against different medium velocities U as indicated in the upper right corner of the images. The trapped bead is shown by an arrow in the first image. (b) Plot of the maximum tube length, L_m, as a function of the flow velocity U. Errors represent the standard deviations over ten measurements. The solid curve is a fit following equation (6), see text for details. The inset shows a fluorescent image of the vesicle with the tube extruded at a medium velocity of $30 \, \mu m \, s^{-1}$. For the staining, the membrane was labeled with 0.1 mol% DiIC18. (c) Retraction of a membrane tube after being extracted using flow velocity $U = 50 \, \mu m \, s^{-1}$. Errors represent standard deviations over ten measurements. The solid curve is a fit following equation (8), see text for details.

the concentration range for curvature generating molecules towards much lower concentrations.

Next, we studied tube retraction. Medium flow velocity of $50 \, \mu m \, s^{-1}$ was first applied to form the tube. After the vesicle has attained the stationary state, the medium flow was quickly stopped to allow the tube to retract while still holding the bead with the optical tweezers. This dynamic process now involves the main counter force from hydrodynamic drag

friction between the rapidly moving internal and external bilayer leaflets as discussed in the context of equation (1). The changing length of the tube was monitored over the time scale of retraction. Figure 2(c) shows the measured tube lengths at 0.2 s time intervals during retraction. The data shown are the averages over ten measurements. They were fitted following equation (8) with b as a fitting parameter and using the estimated values for κ and Σ_0 from figure 2(b), taking $h \cong 2.71$ nm for the thickness of the hydrophobic bilayer [32]. The solid line shows the best fit obtained with interlayer viscosity $b = (3.74 \pm 0.28) \times 10^9 \, N \, s \, m^{-3}$. Similar measurements carried out over five other vesicles yield values for b as $(3.32 \pm 0.73) \times 10^9 \, N \, s \, m^{-3}$. This value is somewhat higher than that measured on lipids with identical hydrophobic chains such as dimyristoylphosphatidylcholine (DMPC) and dioleoylphosphatidylcholine (DOPC) [33]. The slightly higher value of b which we report here most likely reflects partial interdigitation as predicted in reference [33]. Interdigitation is expected for bilayers made of lipids with different chains, such as POPC used in this work.

In systems exhibiting inward membrane tubulation, namely in vesicles with negative spontaneous curvature [34, 35], it is very advantageous if one can pull inward tubes (in the vesicle interior). For this purpose it is required to manipulate the trapped bead across the membrane and take it to the vesicle interior. As shown in figures 3(a)–(d), a trapped bead can be brought into the vesicle interior upon applying fluid flow pressure on the vesicle. To test how the theoretical analysis applies to inward tubes, we used the same vesicle as in figures 1 and 2, for which we had already obtained the initial membrane tension from pulling outward tubes.

After having manipulated the bead inside the vesicle, we could use it to pull inward tubes by dragging the vesicle relative to the trapped bead via controlling the fluid flow. In figures 3(a)–(d), extrusion of an inward tube with a length of approximately 11 μm is shown. The tube is not visible under phase contrast observation, but can be seen in fluorescence, see figure 3(d) (the membrane was stained with DiIC18). Inside the vesicle, the maximum tube length is limited by the vesicle and bead sizes. Applying a flow velocity of $U \cong 30 \, \mu m \, s^{-1}$ we could extrude a tube with maximal length $L_m \cong 16.4 \, \mu m$. Following equation (6), this gives an estimate for the initial membrane tension $\Sigma_0 \cong 1.12 \times 10^{-8} \, N \, m^{-1}$, which is in good agreement with the estimate made from studying outward tubes. When the flow is stopped the tube retracts, dragging the vesicle back onto the trapped bead (figure 3(c)). In figure 3(e), we show the retraction profile of the inwardly pulled tube. The profile follows the logarithmic pattern well as predicted by equation (8), showing similar dynamics as that followed by the external tubes (compare with figure 2(c)). From the retraction profile we could estimate the interlayer slip coefficient as $b = (3.19 \pm 0.38) \times 10^9 \, N \, s \, m^{-3}$, which is again in excellent agreement with results from pulling outward tubes. The values of b obtained from studying six vesicles is $(3.43 \pm 0.71) \times 10^9 \, N \, s \, m^{-3}$. The vesicle diameters during extrusion and retraction of both inward and outward tubes were found to be unchanged within the measurement error of $\pm 0.2 \, \mu m$.

J. Phys. D: Appl. Phys. **47** (2014) 282001

Fast Track Communication
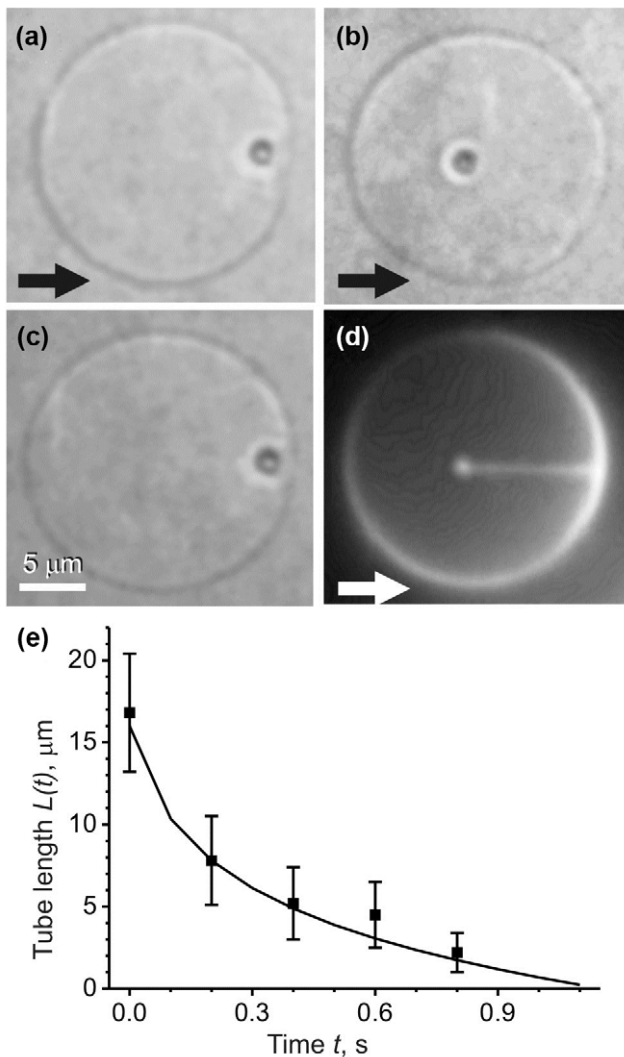
Figure 3. Extrusion and relaxation of inward membrane tubes in a vesicle (same vesicle as in figures 1 and 2). (*a*) The trapped bead is pressed onto and taken inside the vesicle by controlling the fluid flow. (*b*) Using external flow the vesicle is dragged so as to cause separation between the trapped bead and the vesicle membrane so that a tube can be formed. The direction of the flow is shown with arrows. (*c*) The tube retracts when the flow is stopped. (*d*) Fluorescence image of the vesicle using 0.1 mol% DiIC18 staining. The tube is clearly visible. (*e*) Retraction profile of the inward membrane tube. Errors have been estimated as standard deviations over ten measurements. The solid curve is a fit following equation (8), see text for details.

We have shown here that optically trapped beads can be used to investigate free flaccid vesicles with the aid of a controlled medium flow. Theoretical results and experimental studies have been presented to show that the method of pulling inward and outward tubes from vesicles manipulated with a hydrodynamic flow can provide means to estimate several important mechanical parameters of the vesicle membrane simultaneously. The technique can be used to form membrane tubes with directly measurable diameters, enabling estimation of elastic coefficients of the membrane within a single experiment. The results here were obtained on neutrally charged vesicles, but since pulling tubes from GUVs containing charged lipids have been shown to proceed

analogously (see e.g. [36]), we expect that the method is applicable to charged membranes as well. The application of a very minute force of less than a pN to extrude tubes from flaccid vesicles suggests the important potential of this approach for investigating membrane tubulation processes caused by very low concentrations of curvature-active proteins. Most significantly, for the first time membrane tubes in the interior of a vesicle could be extruded and studied, a technique with potentially promising applications in future studies of bending mechanisms in membranes with negative spontaneous curvature.

References

[1] Rafelski S M and Marshall W F 2008 Building the cell: design principles of cellular architecture *Nature Rev. Mol. Cell Biol.* **9** 593–602

[2] Schmidtke D W and Diamond S L 2000 Direct observation of membrane tethers formed during neutrophil attachment to platelets or P-selectin under physiological flow *J. Cell Biol.* **149** 719–29

[3] Davis D M and Sowinski S 2008 Membrane nanotubes: dynamic long-distance connections between animal cells *Nature Rev. Mol. Cell Biol.* **9** 431–6

[4] Rustom A, Saffrich R, Markovic I, Walther P and Gerdes H H 2004 Nanotubular highways for intercellular organelle transport *Science* **303** 1007–10

[5] Csordas G, Renken C, Varnai P, Walter L, Weaver D, Buttle K F, Balla T, Mannella C A and Hajnoczky G 2006 Structural and functional features and significance of the physical linkage between ER and mitochondria *J. Cell Biol.* **174** 915–21

[6] Dimova R, Aranda S, Bezlyepkina N, Nikolov V, Riske K A and Lipowsky R 2006 A practical guide to giant vesicles. Probing the membrane nanoregime via optical microscopy *J. Phys.: Condens. Matter* **18** S1151–76

[7] Dimova R 2012 Giant vesicles: a biomimetic tool for membrane characterization *Advances in Planar Lipid Bilayers and Liposomes* (New York: Academic) pp 1–50

[8] Rossier O, Cuvelier D, Borghi N, Puech P H, Derenyi I, Buguin A, Nassoy P and Brochard-Wyart F 2003 Giant vesicles under flows: extrusion and retraction of tubes *Langmuir* **19** 575–84

[9] Borghi N, Rossier O and Brochard-Wyart F 2003 Hydrodynamic extrusion of tubes from giant vesicles *Europhys. Lett.* **64** 837

[10] Waugh R E 1982 Surface viscosity measurement from large bilayer vesicle tether formation: II. Experiments *Biophys. J.* **38** 29–37

[11] Huang Z H, Abkarian M and Viallat A 2011 Sedimentation of vesicles: from pear-like shapes to microtether extrusion *New J. Phys.* **13** 035026

[12] Bo L and Waugh R E 1989 Determination of bilayer-membrane bending stiffness by tether formation from giant, thin-walled vesicles *Biophys. J.* **55** 509–17

[13] Cans A S, Wittenberg N, Karlsson R, Sombers L, Karlsson M, Orwar O and Ewing A 2003 Artificial cells: unique insights into exocytosis using liposomes and lipid nanotubes *Proc. Natl Acad. Sci. USA* **100** 400–4

[14] Shnyrova A V, Bashkirov P V, Akimov S A, Pucadyil T J, Zimmerberg J, Schmid S L and Frolov V A 2013 Geometric

J. Phys. D: Appl. Phys. **47** (2014) 282001

Fast Track Communication

catalysis of membrane fission driven by flexible dynamin rings *Science* **339** 1433–6

[15] Heinrich V and Waugh R E 1996 A piconewton force transducer and its application to measurement of the bending stiffness of phospholipid membranes *Ann. Biomed. Eng.* **24** 595–605

[16] Koster G, Cacciuto A, Derényi I, Frenkel D and Dogterom M 2005 Force barriers for membrane tube formation *Phys. Rev. Lett.* **94** 068101

[17] Cuvelier D, Derenyi I, Bassereau P and Nassoy P 2005 Coalescence of membrane tethers: experiments, theory, and applications *Biophys. J.* **88** 2714–26

[18] Baumgart T, Capraro B R, Zhu C and Das S L 2011 Thermodynamics and mechanics of membrane curvature generation and sensing by proteins and lipids *Annu. Rev. Phys. Chem.* **62** 483–506

[19] Karlsson M, Sott K, Cans A S, Karlsson A, Karlsson R and Orwar O 2001 Micropipet-assisted formation of microscopic networks of unilamellar lipid bilayer nanotubes and containers *Langmuir* **17** 6754–8

[20] Gauthier N C, Masters T A and Sheetz M P 2012 Mechanical feedback between membrane tension and dynamics *Trends Cell Biol.* **22** 527–35

[21] Diz-Muñoz A, FletcherD A and Weiner O D 2013 Use the force: membrane tension as an organizer of cell shape and motility *Trends Cell Biol.* **23** 47–53

[22] Mattila P K, Pykäläinen A, Saarikangas J, Paavilainen V O, Vihinen H, Jokitalo E and Lappalainen P 2007 Missing-in-metastasis and IRSp53 deform PI(4,5)P2-rich membranes by an inverse BAR domain–like mechanism *J. Cell Biol.* **176** 953–64

[23] Evans E and Yeung A 1994 Hidden dynamics in rapid changes of bilayer shape *Chem. Phys. Lipids* **73** 39–56

[24] Dimova R, Seifert U, Pouligny B, Förster S and Döbereiner H-G 2002 Hyperviscous diblock copolymer vesicles *Eur. Phys. J.* E **7** 241–50

[25] Kraikivski P, Pouligny B and Dimova R 2006 Implementing both short- and long-working-distance optical trappings into a commercial microscope *Rev. Sci. Instrum.* **77** 113703

[26] Dasgupta R, Verma R S and Gupta P K 2012 Microfluidic sorting with blinking optical traps *Opt. Lett.* **37** 1739–41

[27] Angelova M I and Dimitrov D S 1986 Liposome electroformation *Faraday Discuss.* **81** 303–11

[28] Schneider C A, Rasband W S and Eliceiri K W 2012 NIH Image to ImageJ: 25 years of image analysis *Nature Methods* **9** 671–5

[29] Pontes B, Viana N B, Campanati L, Farina M, Neto V M and Nussenzveig H M 2008 Structure and elastic properties of tunneling nanotubes *Eur. Biophys. J. Biophys. Lett.* **37** 121–9

[30] Dimova R 2014 Recent developments in the field of bending rigidity measurements on membranes *Adv. Colloid Interface Sci.* **208** 225–34

[31] Weast R 1988 *Handbook of Chemistry and Physics* (Boca Raton: CRC Press)

[32] Kucerka N, Tristram-Nagle S and Nagle J F 2005 Structure of fully hydrated fluid phase lipid bilayers with monounsaturated chains *J. Membr. Biol.* **208** 193–202

[33] Merkel R, Sackmann E and Evans E 1989 Molecular friction and epitactic coupling between monolayers in supported bilayers *J. Phys.* **50** 1535–55

[34] Li Y, Lipowsky R and Dimova R 2011 Membrane nanotubes induced by aqueous phase separation and stabilized by spontaneous curvature *Proc. Natl Acad. Sci. USA* **108** 4731–6

[35] Lipowsky R 2013 Spontaneous tubulation of membranes and vesicles reveals membrane tension generated by spontaneous curvature *Faraday Discuss.* **161** 305–31

[36] Waugh R E, Song J, Svetina S and Zeks B 1992 Local and nonlocal curvature elasticity in bilayer-membranes by tether formation from lecithin vesicles *Biophys. J.* **61** 974–82